Check for updates

# Porewater exchange drives the dissolved silicate export across the wetland-estuarine continuum

Fenfang Wang[1,2], Zeyang Lu[1,2], Yao Wang[1], Ruifeng Yan[1] and Nengwang Chen[1,2]*

[1]Fujian Provincial Key Laboratory for Coastal Ecology and Environmental Studies, College of the Environment and Ecology, Xiamen University, Xiamen, China, [2]State Key Laboratory of Marine Environmental Science, Xiamen University, Xiamen, China

Coastal wetlands are an important hotspot for nutrient cycling and transport from the land to the ocean. Silicon (Si) as a vital biogenic element affects plant growth and health of coastal ecosystems. The understanding of key factors and processes controlling dissolved silicate (DSi) exchange between the wetlands and coastal water has been limited due to the lack of measured data. We carried out intensive investigations of time-series DSi concentrations and porewater exchange across the Sediment-Water Interface (SWI) along a tidal creek with a mangrove-salt marsh gradient during neap and spring tides in 2020. Seasonal observations of surface water in a tidal creek and Zhangjiang Estuary (Fujian Province, China) were conducted from 2017 to 2020. The results showed that there was a net export of DSi from the mangroves to tidal creek with rates of 2.11 and 2.40 mmol m^{-2} d^{-1} in neap and spring tides respectively, suggesting the mangroves served as the source of DSi. However, the salt marshes had a net DSi import with one or two orders of magnitude lower than the export from the mangroves. DSi export across the wetland-estuarine continuum was largely controlled by porewater exchange, groundwater geochemistry (pH, temperature) and plant root uptake. Groundwater in the mangroves has larger ratios of DSi : DIN (dissolved inorganic nitrogen) (2.5 ± 0.6) and DSi : DRP (dissolved reactive phosphorus) (1257 ± 35) compared with surface water. The net export of DSi from mangroves would modify the nutrient stoichiometry and mitigate the effects of reduced river DSi flux caused by damming on coastal ecosystem. This study provides new insights into the wetland Si cycling for sustaining coastal ecosystem health.

KEYWORDS

nutrient fluxes, mangrove, salt marsh, coastal water quality, Zhangjiang Estuary

GRAPHICAL ABSTRACT
Conceptual schematic
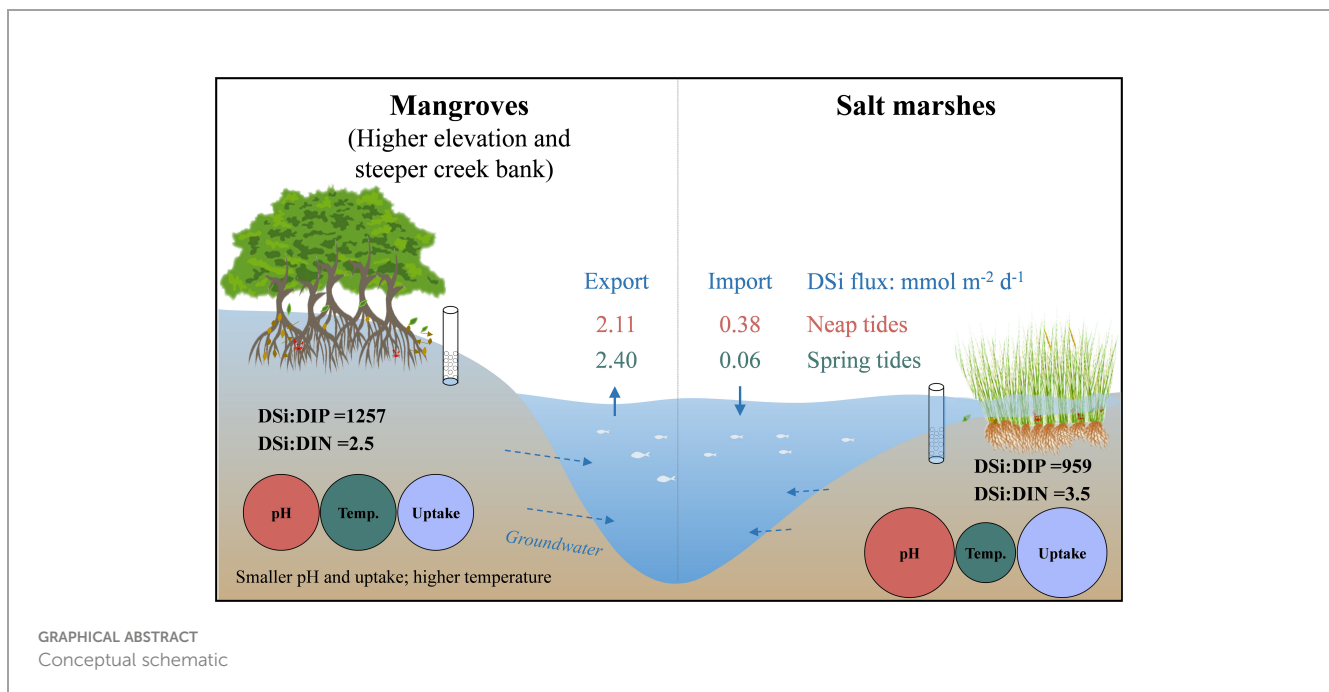
Highlights:

- DSi export from wetlands to estuary driven by porewater exchange was explored.
- Mangroves had a large net export of DSi but salt marshes had a minor import.
- DSi export from mangroves would mitigate effects of reduced river DSi by dam.

1 Introduction

Mangroves are known as a critical "blue carbon" system with high productivity of 635 Tg C yr^{-1} and large carbon storage of 739 Mg ha^{-1} (Alongi, 2014; Alongi, 2020). Nitrogen (N) and phosphorus (P) cycling and transport in mangroves and adjacent estuary have been well studied, revealing wetland's positive or negative effects on coastal ecosystems (Wang et al., 2019; Wang et al., 2021). Silicon (Si, the second most abundant element in the earth's crust) is an important element for wetlands and marine ecosystems (Epstein, 1994; Ma and Takahashi, 2004). Many studies focused on Si concentrations, compositions and their variations in plants and sediments (de Bakker et al., 1999; Elizondo et al., 2021). However, the export-import pattern of dissolved silicate (DSi) in mangrove wetlands was rarely studied. In some parts of the world, such as Asia, Africa, Australia, and N. America, mangroves are invading salt marshes with warming climate (Saintilan et al., 2014). In China, the Spartina alterniflora, a type of salt marshes with high tolerance to salinity and hypoxia, strong capacity for competitiveness, is invading the native mangroves or mudflats, forming a mangrove-salt marsh coexistent ecotone (Li et al., 2009; Zhang et al., 2012; Wang and Lin, 2023). The potential effects of salt marsh invasion on DSi export-import patterns in native wetlands have received little attention.

Wetlands have been recognized as "hot spots" for Si cycling due to the critical role in Si transport and processing (Struyf and Conley, 2009). Plants are efficient in taking up and storing Si, and also release Si into the sediments supporting further biogeochemical cycling (Hou et al., 2010; Liang et al., 2015). Si is involved in the nutrient cycling, organic matter degradation and carbon storage (Xia et al., 2020). This biogeochemical processes about Si in wetlands determined the form and amount available for exchange with coastal ecosystems. The land-ocean fluxes of DSi are controlled by the geochemical, biological, and hydrodynamic processes (Cornelis et al., 2010). The sources or sinks of Si in the wetland ecosystem have been studied with inconsistent conclusion. A study based on sequential extractions of Si and Fe, modeling of the soil aqueous phase, and X-ray diffraction of the fine clay fraction showed that the hypersaline tidal flat soils tend to be the sink of Si due to the adsorption, (co)precipitation, and reactions involving clay minerals (Sartor et al., 2019). The study in Gazi Bay with the growth of mangroves and seagrasses showed that benthic fluxes were the major source of Si^{4+} with larger fluxes in mangrove than in seagrass, which play a significant role in the functional understanding and protection and restoration of the coastal wetlands (Mwashote and Jumba, 2002). However, the underlying mechanisms controlling DSi export-import pattern in wetlands are still unknown.

Dams are recognized as "in-stream" reactors to impede nutrient transport (Maavara et al., 2020b), altering DSi fluxes along the land-ocean aquatic continuum by retention (Laruelle et al., 2009; Harrison et al., 2012; Chen et al., 2014). A study in the Jiulong River, Southeast China, showed that dam retention caused a 16% decrease in DSi flux (Chen et al., 2014). Studies based on nutrient cycling and mechanistic model predicted that dams will retain 5.3% of global reactive silicon, and more than half of rivers will experience greater removal of Si over N and P by the midcentury (Maavara et al., 2014; Maavara et al., 2020a). The decreased DSi flux from the land to the ocean has altered nutrient stoichiometry and phytoplankton structures, increasing the

risk of non-diatom bloom (Li et al., 2019). Our companion research has explored the N and P source-sink pattern in a mangrove-salt marsh-estuary system driven by the porewater exchange and nutrient cycling (Wang et al., 2022b). Under the scenario of a decrease in land-ocean silica fluxes caused by river damming, it is crucial to obtain a better insight into the role of wetlands in the Si transport between land and ocean. Here, we assume wetlands have potential to increase DSi export and the increased fluxes will mitigate the negative effects of reduced global river Si on marine ecosystem caused by worldwide damming.

The porewater or groundwater exchange (PEX) is recognized as a major pathway for material transport from the land to the ocean (Chen et al., 2019; Santos et al., 2019; Santos et al., 2021; Hu et al., 2022). The contributions of Si fluxes driven by PEX to total Si fluxes differed in heterogeneous environments with the contributions of 14-32% in the Jiulong River Estuary, 5% in a salt marsh of the Changjiang River Estuary, China, and 58-90% in the Krka River Estuary characterized as oligotrophy (Wang et al., 2015; Liu et al., 2019; Chen et al., 2021). Tides are recognized as a major control for Si fluxes by affecting hydraulic gradient, hydraulic retention time and wave setup (Moore, 1996; Taniguchi, 2002). Studies based on high-resolution time-series observation suggested the water parameters such as salinity, pH, and redox potential varied with tides, and thus affected the microbial activities, nutrient cycling, the distribution of reduced species and the elemental adsorption and desorption (Taniguchi, 2002; Delgard et al., 2012). The exploration of hydrogeological impacts is crucial to understand Si export or import in wetlands.

Herein, we focused on the spatial and temporal distribution of DSi and vertical DSi fluxes across the Sediment-Water Interface (hereafter "SWI") in a subtropical mangrove wetland system invaded by the salt marshes. We conducted seasonal observations in the mangrove-salt marsh-tidal creek-Zhangjiang Estuary continuum from 2017 to 2020. Two time-series observations of physicochemical parameters and DSi concentrations in surface water and groundwater were conducted during a spring-neap tidal cycle in 2020. The specific objectives of this study were to: (1) explore the seasonal and spatial variations of DSi concentration across the mangrove-salt marsh creek-estuary continuum; (2) estimate DSi fluxes across the SWI in the mangroves and salt marshes; (3) reveal the key factors and processes controlling DSi export-import pattern in the mangrove-salt marsh ecotone.

2 Materials and methods

2.1 Description of the study site

The study was conducted in a National Mangrove Reserve and the adjacent Zhangjiang Estuary (117°24′-117°30′E, 23°53′-23°56′N) in Southeast China (Figure 1). The dominant mangrove species are *Kandelia candel*, *Avicennia marina* and *Aegiceras corniculatum* with a total area of 2.6 km^2 (Zhou et al., 2010). The wetlands experience a semidiurnal tide with a tidal range of 0.43-4.67 m, and a subtropical monsoon climate with an annual mean temperature of 22.8 ± 5.7°C and precipitation of 1,679 mm (Wang et al., 2019). The salt marshes (mainly *Spartina alterniflora*) have invaded mudflat areas with an expansion on the edge of mangroves. Zhangjiang

Estuary, connected with wetlands, has a length of 58 km with a watershed area of 855 km^2.

2.2 Sampling campaigns and chemical analysis

The seasonal observations in the mangrove-salt marsh creek-Zhangjiang Eestuary continuum were carried out from 2017 to 2020. Surface water samples (0.5 m) were collected along the route from the mangrove-salt marsh creek to the adjacent estuary (Figure 1B). The samples in tidal creek were collected in flood and ebb tides and those in the estuary were collected at high tides (the periods of flood, ebb and high tides were shown in Figure S1). Surface water samples were collected during the monitoring periods using a Niskin hydrophore.

Two fixed sites along the creek edges of the mangroves and salt marshes (Figure 1C) were chosen to conduct time-series measurements (25 h) of surface water (0.5 m) and groundwater during neap tides on 11th-12th October and spring tides on 20th-21st October 2020, respectively. A "paired-wells" device (70 cm) equipped with two CTD-Diver loggers (vanEssen, Netherlands) was installed in the creek edge sediments. Water temperature, conductivity and pressure were recorded using upper (5 cm) and lower (65 cm) loggers at a frequency of 30 minutes to quantify PEX rates (See the schematic diagram of the device in Figure S2). The monitoring began two days after installation to minimize the impact of sediment disturbance. Surface water samples were collected hourly in whole tidal cycles using a Niskin hydrophore. Groundwater samples were collected hourly at low tides using a peristaltic pump.

Water samples were filtrated immediately in the field with a GF/F membrane (0.7 μm) and stored at 4°C until analysis. The concentrations of ammonium (NH$_4$-N), nitrate (NO$_3$-N), nitrite (NO$_2$-N), dissolved reactive phosphorus (DRP) and DSi were analyzed using segmented flow colorimetry (San++ analyzer, Germany) (Detailed about the measurement method are showed in Text S1). Dissolved inorganic nitrogen (DIN) was the sum of NH$_4$-N, NO$_3$-N and NO$_2$-N. Salinity, pH, dissolved oxygen (DO) concentration, and temperature were measured in-situ using a multiparameter portable meter (Multi WTW 3430, Germany).

2.3 DSi offset and PEX rate

The DSi offset of a mangrove creek in ebb tides from the conservative mixing line of the estuary was calculated with equations (1) and (2).

$$DSi_{Exp} = ax + b \qquad (1)$$

$$DSi_{Offset} = DSi_{Obs} - DSi_{Exp} \qquad (2)$$

where DSi$_{Offset}$ is DSi offset from the mixing lines of the estuary (μmol L^{-1}); a and b is the slope and intercept of the mixing line, respectively; x is the observed salinity in tidal creek in ebb tides; DSi$_{Exp}$ and DSi$_{Obs}$ is the calculated and observed concentration in tidal creek (μmol L^{-1}), respectively.
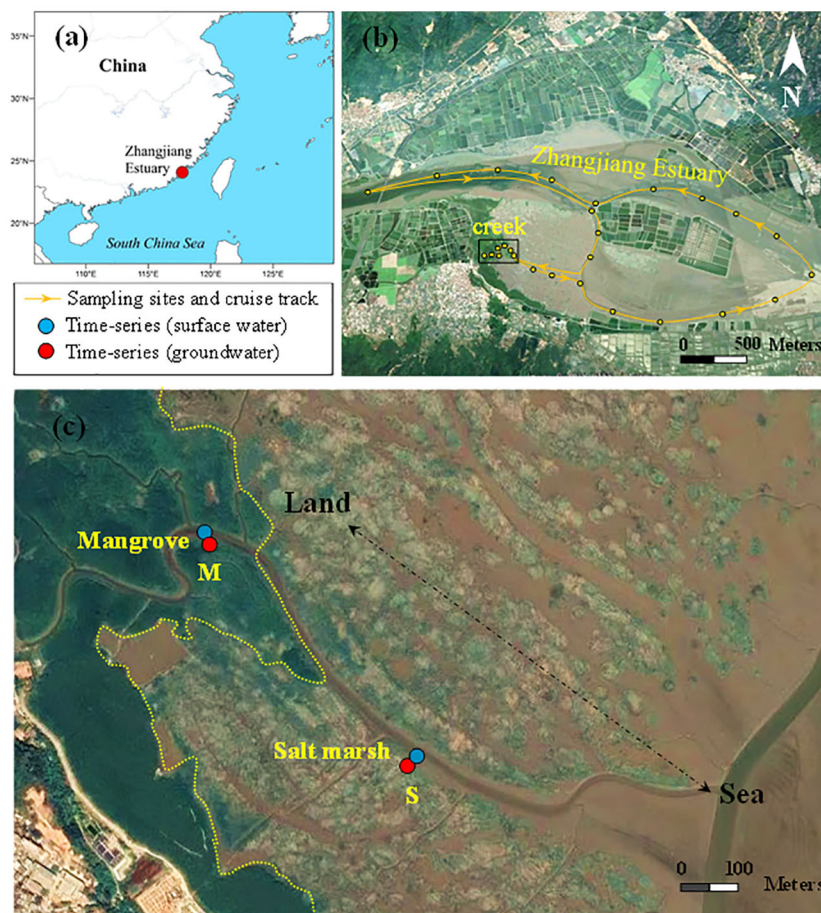
FIGURE 1
Study area and sampling sites (modified from Wang et al., 2022b). **(A)** The location of the study area to the South China Sea. **(B)** The sampling sites along the mangrove tidal creek and Zhangjiang Estuary. A line with arrows indicates the cruise track and direction. **(C)** The time-series observation sites of surface water and groundwater in the mangroves (M, left area of the yellow line) and salt marshes (S, right area of the yellow line).

Linear regression was carried out to analyze the relationship between DSi offset and tidal range in ebb tides.

The vertical PEX rate was calculated by the hydraulic gradient and vertical hydraulic conductivity, which were based on the generalized form of Darcy's law and in-situ falling head method, respectively. See more details in supporting information (Text S2).

3 Results

3.1 Spatial and temporal variations of DSi

DSi showed spatial variations in mangrove-salt marsh tidal creek-estuary continuum (Figure 2 and Table 1). The average concentration of DSi in the estuary was 154 ± 37 μmol L^{-1}. In salt marsh creek, the average concentration in flood and ebb tides was similar to or slightly larger than in the estuary. In mangrove creek, the average concentration in ebb and flood tides was 19% and 14% larger than in the estuary.

DSi-salinity diagrams showed that DSi had a mostly conservative behavior against salinity gradient in the estuary (Figure 2). DSi in mangrove creek in flood tides, and in salt marsh creek in both flood and ebb tides were nearly on the mixing line. In ebb tides, DSi in mangrove creek was larger than those in the estuary at a given salinity with the exceptions in autumn 2017 (October) and 2019 (November). There was a strong positive correlation ($R^2 = 0.58$, $p<0.05$) between DSi offset and tidal range in the mangrove creek in ebb tides (Figure 3).

3.2 Time-series physicochemical parameters and DSi concentrations

Water depth during spring tides (0.68-3.93 m) was larger than during neap tides (0.85-3.28 m) (Figure 4). The average pH values during neap and spring tides of mangrove groundwater (6.86 ± 0.14) were smaller than those of salt marsh groundwater (7.44 ± 0.08). The average temperature of mangrove groundwater (27.5 ± 1.8°C) was higher than of salt marsh groundwater (25.4 ± 1.9°C). The salinity and DO of salt marsh groundwater were larger than those of mangrove groundwater (Figure 4; See more details in Wang et al., 2022b).

The DSi concentrations varied with tidal cycles, water types, and habitats (Figure 4 and Table 2, S1). During neap tides, the average DSi concentration at low tides was 10% higher than at high tides in mangrove surface water (Figure 4), and the average DSi
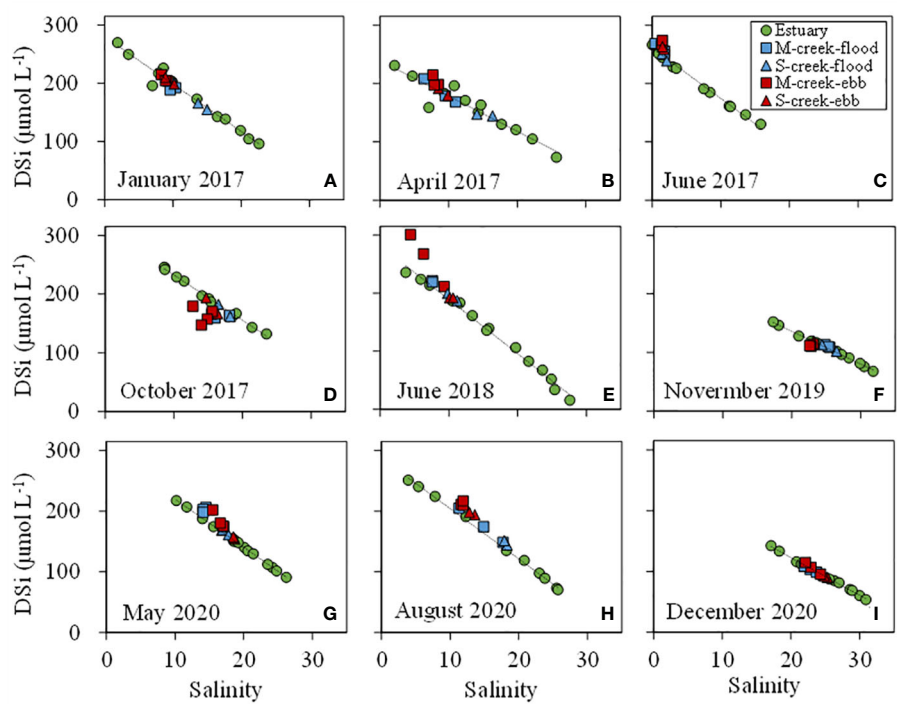
FIGURE 2
Diagrams of DSi against salinity (2017-2020). The squares and triangles indicate the concentrations in mangrove (M, blue) and salt marsh (S, red) creek in flood and ebb tides, respectively. The green circles mean the concentrations in Zhangjiang Estuary, showing a conservative mixing (black dotted line) along the salinity gradient.

concentration in groundwater was 43% higher than in surface water (Table 2). In the salt marshes, the DSi concentration at low tides was 3% higher than at high tides (Table S1), and the average concentration was 31% higher in groundwater than in surface water (Table 2). During spring tides, DSi concentrations were lower than during neap tides in both the mangroves and salt marshes with an exception in mangrove groundwater, which was 39% higher than during neap tides (Figure 4). The DSi concentration at low tides was 19% and 7% larger than at high tides in the mangroves and salt marshes, respectively (Table S1). In

the mangroves, the DSi concentration in groundwater was twice as high as during neap tides, 69% larger than in surface water (Figure 4 and Table 2). In the salt marshes, the DSi concentration in groundwater was similar to in surface water, much smaller than in mangrove groundwater (Table 2).

The DIN and DRP concentrations varied with water types and habitats (Figure S3). In mangroves, the DIN concentrations in surface water was similar during spring (76 ± 14 µoml L^{-1}) and neap tides (74 ± 7 µoml L^{-1}), 64% and 20% smaller than in groundwater. The average DIN in salt marsh surface water (71 ±

TABLE 1 The DSi concentration (Mean ± SD) in mangrove (M) and salt marsh (S)-tidal creek, and estuary in flood and ebb tides.

| Date	DSi (µmol L^{-1})				
	M-creek-flood	S-creek-flood	Estuary	M-creek-ebb	S-creek-ebb
2017.01.13	193 ± 5	160 ± 8	180 ± 56	208 ± 6	204 ± 8
2017.04.28	185 ± 21	146 ± 2	158 ± 45	203 ± 10	185 ± 8
2017.06.22	258 ± 10	245 ± 8	212 ± 48	269 ± 4	261 ± 3
2017.10.31	163 ± 3	172 ± 15	197 ± 40	164 ± 14	180 ± 19
2018.06.30	222 ± 4	193 ± 9	139 ± 76	260 ± 45	192 ± 0
2019.11.17	111 ± 3	108 ± 8	108 ± 27	112 ± 2	118 ± 3
2020.05.27	205 ± 5	166 ± 4	147 ± 37	183 ± 13	156 ± 2
2020.08.17	176 ± 28	148 ± 5	149 ± 71	213 ± 4	196 ± 3
2020.12.17	103 ± 5	92 ± 2	93 ± 28	106 ± 10	91 ± 2
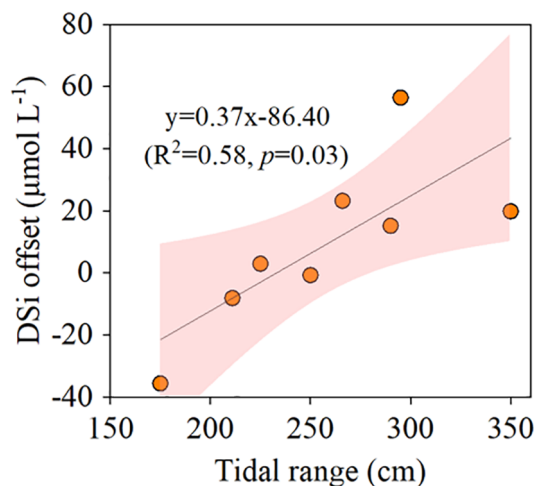
FIGURE 3
The relationship between tidal range and DSi offset from conservative mixing line of estuary in mangrove creek in ebb tides during 2017-2020 (refer to Figure 2). The pink shaded area means 95% confidence band.

1 µoml L^{-1}) was close to that in mangrove surface water (75 ± 1 µoml L^{-1}), but DIN in salt marsh groundwater (56 ± 20 µoml L^{-1}) was 63% smaller than in mangrove groundwater (152 ± 84 µoml L^{-1}). The DRP concentrations in mangrove groundwater was 5-15 times smaller than in surface water (Figure S3). DRP in surface water and groundwater in salt marshes were lower than that in mangroves during neap tides. During spring tides, DRP was similar in salt marsh surface water and groundwater, both higher than that during neap tides.

The ratios of DSi : DIN (dissolved inorganic nitrogen) ranged from 1.77 to 2.12 and 2.07 to 4.98 in surface water and groundwater, respectively (Table 2). The ratios were 29% and 14% larger in mangrove groundwater, and 57% and 15% larger in salt marsh groundwater than in their surface water during neap and spring tides. The ratios of DSi : DRP (dissolved reactive phosphorus) ranged from 58 to 167 and 89 to 1829 in surface water and groundwater, respectively (Table 2). The DSi : DRP ratios were 96% and 94% larger in mangrove groundwater, and 91% and 30% larger in salt marsh groundwater than in their surface water during neap and spring tides.

3.3 PEX and DSi fluxes

The PEX across SWI varied with tidal types and habitats (Figure S2). In the mangroves, the average outflow rates during neap and spring tides were 0.75 and 0.41 mm h^{-1}, much larger than inflow rates (0.20 mm h^{-1} during both neap and spring tides). In the salt marshes, the outflow rates of groundwater were close to the inflow rates of surface water during spring tides. The inflow rate (0.26 mm h^{-1}) was 42% larger than the outflow rate during neap tide.

The magnitude and direction of DSi fluxes across SWI varied with tidal types and habitats (Figure 5). DSi was exported from groundwater to surface water at low tides, while was imported to groundwater from surface water at high tides in both the mangroves and salt marshes. In the mangroves, DSi had a net export, and the efflux during spring tides (2.40 mmol m^{-2} d^{-1}) was 10% larger than during neap tides (2.11 mmol m^{-2} d^{-1}) (Figure 5). In the salt marshes, DSi had a net import, and the influx during neap tides (0.38 mmol m^{-2} d^{-1}) was larger than during spring tides (0.06 mmol m^{-2} d^{-1}) (Figure 5), both much smaller than the efflux in the mangroves.

4 Discussion

4.1 Hydrological controls on DSi export or import

Tides are recognized as a key factor controlling material transport from wetlands to coastal areas (Liu et al., 2017; Wang et al., 2019). DSi-salinity relationship showed that DSi in mangrove creek in ebb tides mostly fell above the conservative mixing lines of the estuary while fell on the mixing lines in flood tide (Figure 2). This suggested the groundwater discharge from mangrove sediments affected DSi concentration in the tidal creek in ebb tides, while seawater played a leading role in flood tides. The DSi concentrations in salt marsh creek fell on or slightly above the mixing lines in both flood and ebb tides (Figure 2), suggesting the groundwater discharged from salt marsh sediments played a minor role in the creek water. The significant positive relationship between DSi offset and tidal range in the mangroves suggested the control of tidal pumping on the groundwater discharge from the sediments to tidal creek (Figure 3). This was consistent with a previous study showing that porewater exchange significantly contributes to the mangrove source function of dissolved metal, carbon, and nutrient driven by tidal pumping (Sadat-Noori and Glamore, 2019).

The PEX was controlled by the hydraulic conductivity of sediments and hydraulic gradient (Santos et al., 2014; Oh et al., 2020). Salt marshes had a smaller PEX than the mangroves, and the vertical hydraulic conductivity in the salt marsh was slightly larger but the hydraulic gradient was smaller than in the mangroves (Figure S2), suggesting the hydraulic gradient played a more important role in the salt marsh PEX. The larger hydraulic gradient caused by a larger slope of creek bank (22% larger than the salt marshes) and higher surface elevation resulted in a larger PEX in the mangroves (Figure S2). A larger hydraulic gradient during neap tides explained larger net groundwater efflux in the mangroves. All of these demonstrated the hydrological controls on the PEX difference between the mangroves and salt marshes in this study area.

4.2 Contrasting DSi fluxes across SWI between the mangroves and salt marshes

The DSi concentration in porewater of sediments was the net result of equilibrium between the uptake and restitution of Si (Street-Perrott and Barker, 2008). Plants take up Si from porewater released by weathering of mineral or phytolith and
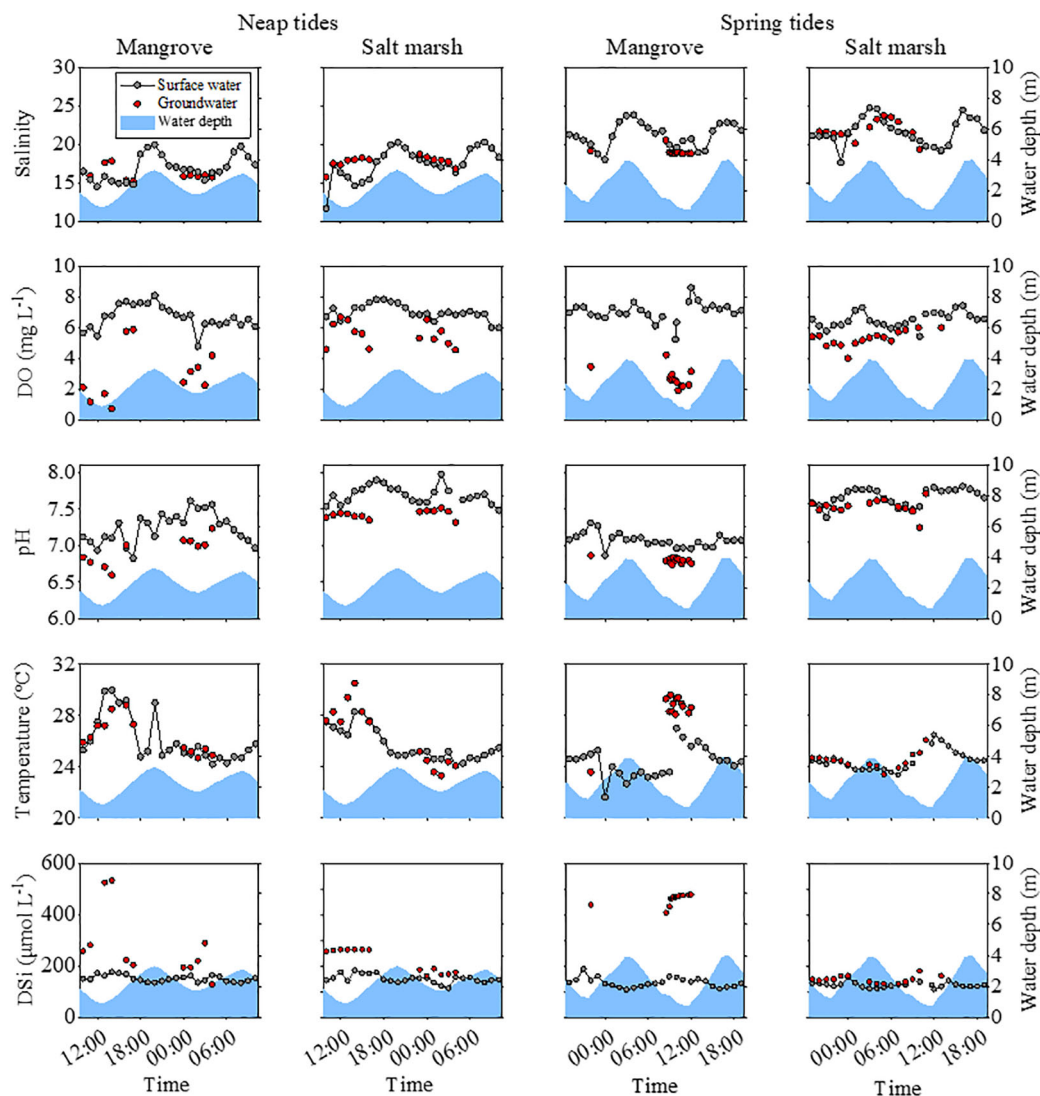
FIGURE 4
Tidal variations of water depth, salinity, DO concentrations, pH values, temperature and DSi concentrations in surface water (grey circles) and groundwater (red circles) in the mangroves and salt marshes during neap tides (11th-12th October 2020) and spring tides (20th-21st October 2020). The data on water depth, salinity and DO was derived from our companion article (Wang et al., 2022b).

TABLE 2 Mean (± SD) DSi, ratios of DSi : DIN and DSi : DIP in surface water (SW) and groundwater (GW) in the mangroves (M) and salt marshes (S) during neap tides (11th-12th October 2020) and spring tides (20th-21st October 2020).

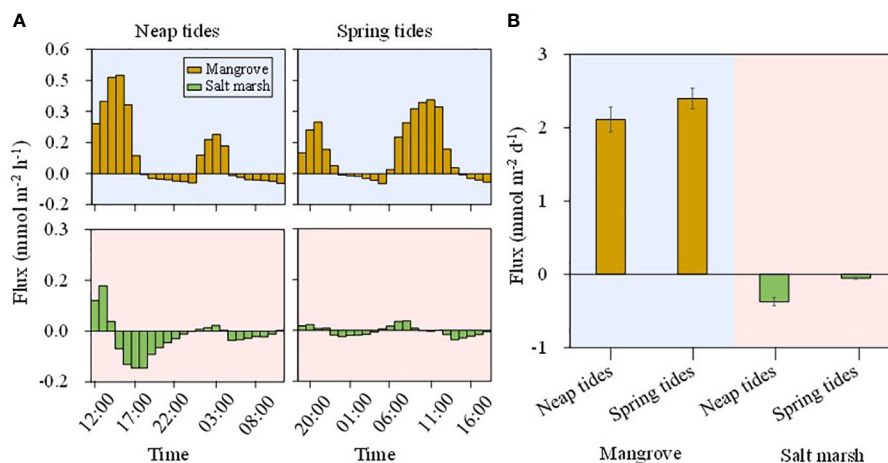| Tidal types	Water types	DSi (μmol L^{-1})	DSi : DIN	DSi : DIP
Neap tides	SW-M	151 ± 13	2.04	59
	GW-M	266 ± 124	2.88	1505
	SW-S	149 ± 16	2.12	167
	GW-S	217 ± 48	4.98	1829
Spring tides	SW-M	135 ± 19	1.77	64
	GW-M	436 ± 94	2.07	1009
	SW-S	126 ± 10	1.77	62
	GW-S	147 ± 14	2.09	89

FIGURE 5
Hourly DSi fluxes **(A)** and net DSi fluxes **(B)** across the SWI in the mangroves (orange bars) and salt marshes (green bars) during neap tides (11th-12th October 2020) and spring tides (20th-21st October 2020). The positive and negative values indicate the export of groundwater and the import of surface water, respectively.

seawater during the submerged periods *via* the transport by roots and stem, and then stored them as the biogenic silica (BSi) (Raven, 2003; Yang and Zhang, 2018). A substantial reactive BSi can return to wetland sediments with litterfall, increasing DSi concentrations *via* mineralization and weathering (Cornelis et al., 2011; Elizondo et al., 2021). The monocots are recognized as the typical Si-accumulators due to the strong uptake of Si (Ma and Takahashi, 2002). Previous studies showed wetlands dominated by grasses accumulate large amounts of Si compared to other plants, including the mangroves (Epstein, 2001; Hodson et al., 2005). The salt marshes, one type of monocots, likely had a higher Si uptake than mangrove plants, which resulted in lower DSi concentrations in salt marsh groundwater than in mangrove groundwater (Figure 4 and Table 2). The BSi pool in the sediments includes the phytoliths and micro-organism remnants (Sauer et al., 2006; Aoki et al., 2007). The organic matter contents in salt marsh sediments were smaller than in native mangrove sediments, and the labile compound in the salt marshes was richer than in the mangroves in this study area (Gao et al., 2018; Wang et al., 2022a), which likely resulted in less accumulation of phytoliths, and further led to lower DSi in salt marsh groundwater *via* weathering (Figure 4 and Table 2).

The dissolution of Si was also determined by environmental factors of sediments or porewater. The pH affect the dissolution of carbonate phase and the liberation of loosely bound silicon (Kellermeier et al., 2012). Previous studies found DSi concentrations increase with pH decrease in the pH range of 4-9 (Qin and Weng, 2006). The significant negative correlation between pH and DSi in the groundwater ($p<0.01$) demonstrated the strong effects of pH on Si dissolution (Figure S4). Mangroves absorb sulfate ion from sediments during growth and accumulate it in the body as sulfide (Gong and Zhang, 1994). The sulfur accumulated in the sediments with the litter fall degradation can be transferred into hydrogen sulfide (H_2S), leading to the decrease of pH in mangrove sediments. The oxidation of pyrite (one of the important products

of mangrove residue decompositions) also increased hydrogen ion concentrations of in mangrove groundwater (Ferreira et al., 2007). Furthermore, the mangroves (especially species from the Rhizophoraceae), are characterized by large amounts of tannins (Zhang and Laanbroek, 2020), which was also a key source of acidity substances in mangrove sediments. These explained more acidic environments of mangrove groundwater than salt marsh groundwater, which supported larger DSi concentrations in mangrove groundwater (Figure 4 and Table 2).

The effect of temperature on weathering and dissolution processes is significant (Rickert et al., 2002). The study in the marine system showed that bacterial activities could accelerate BSi dissolution, and this process was closely related to the water temperature (Bidle and Azam, 1999; Bidle et al., 2002). The DSi concentrations were positively correlated to temperature in this study ($p<0.01$) (Figure S5). Our previous study showed that the inundation time of the mangroves was shorter than salt marshes without obvious difference between neap and spring tides (Wang et al., 2022b). Longer duration of sun exposure of mangrove sediments due to higher elevation and shorter flooding time explained higher temperature in mangrove groundwater (Figure 4), which was conducive to promoting Si dissolution. Moreover, higher temperature promotes microbial activities and respirations in mangrove sediments, which also resulted in lower pH values and larger DSi concentrations than salt marshes (Jin et al., 2013; Liu et al., 2018).

The DSi fluxes were determined by DSi concentrations and PEX across SWI. The mangroves had a net export of DSi during both neap and spring tides (Figure 5) due to larger DSi concentrations in groundwater and larger groundwater outflow than surface water inflow rates (Figure S2). Though a larger hydraulic gradient caused by the low water level resulted in a larger groundwater discharge during neap tides (Figure S2), a 69% larger concentration in groundwater than surface water resulted in a larger net DSi efflux in spring tides than neap tides (Figure 5). In the salt marshes, the

minimal difference in DSi concentrations and water flow rates between surface water and groundwater during spring tides caused DSi efflux and influx to be almost in balance. Though DSi concentration in groundwater was greater than in surface water, the surface water inflow was 42% larger than groundwater outflow during neap tides, resulting in a net DSi influx. This suggested that hydrodynamics played a more important role than the biological and chemical processes in salt marshes. The net fluxes suggested that the mangroves acted as a source of DSi while the salt marshes served as a sink in our study area. The positive DSi offset of mangrove creek from the mixing line was another strong evidence for the view that the mangroves mostly served as the source of DSi relative to estuary (Figures 2, 3).

4.3 Uncertainty analysis

The DSi concentrations showed seasonal variations in mangrove and salt marsh creek (Figure 2) due to the seasonal differences in temperature, rainfall and plant periodicity growth. Our previous study in the same area showed that the nutrient (especially nitrogen) concentrations in tidal creek were affected seriously by the porewater discharged from mangroves in the ebb tides (Wang et al., 2019). The DSi concentrations in mangrove tidal creek showed a similar pattern to nitrogen in this study (Figures 2, 3) in ebb tides, and thus we regarded the creek water in ebb tides as the groundwater, and the creek water in flood tides as the surface water to analyze seasonal DSi fluxes across SWI in the mangroves and salt marshes. The results showed that mangroves always had net DSi effluxes during both neap and spring tides (Figures 6A, B). Salt marshes almost had net DSi influxes with the exception in January, April 2017 and August 2020, and the influxes were one or two orders of magnitude lower than the effluxes in the mangroves. The seasonal export-import pattern was consistent with the pattern derived from time-series observations (Figures 5, 6). Though the uncertainty analysis supported the result that the mangroves were a source while the salt marshes were a sink of DSi, more seasonal field observations are needed in future work to gain more insights into the seasonal DSi source-sink patterns in the wetland-estuarine system.

Horizontal advection in the coastal area is recognized as an important contributor to groundwater discharge (Lara et al., 2012; Coluccio et al., 2021). Previous studies found the ratios of the vertical hydraulic conductivity (K_v) to the horizontal hydraulic conductivity (K_h) of the sediments ranged from 2/3 to 4 in coastal areas (Hughes et al., 1998; Xiao et al., 2017). We estimated the horizontal fluxes of DSi using the average ± SD (2 ± 1) of $K_v : K_h$ mentioned above in the mangroves and salt marshes.

Horizontal flux contributed less to the total flux and did not change DSi source-sink pattern of the mangroves (Table S3). DSi was exported to tidal creek from mangrove and salt marsh sediments *via* the horizontal advection during both neap and spring tides (Table 3). The horizontal flux in the mangroves with a larger slope was greater than in the salt marshes with a smaller slope, which was consistent with a study showing the sloping peatland had a stronger lateral groundwater gradient than the basin peatland (Millar et al., 2018). In the mangroves, the horizontal efflux was much smaller than the vertical efflux, contributing to 23-26% of the total efflux. Nevertheless, the horizontal efflux was almost the same as the vertical influx during neap tides, while 50% greater than the vertical influx during spring tides in the salt marshes (Table 3). As a result, the salt marshes shifted from net import (sink) to net export (source) of DSi. Both the net fluxes with or without horizontal flux in the salt marshes were one or two orders of magnitude smaller than the net efflux of the mangroves, indicating the effects of salt marsh invasion on DSi export from mangrove wetlands to Zhangjiang Estuary is very limited.
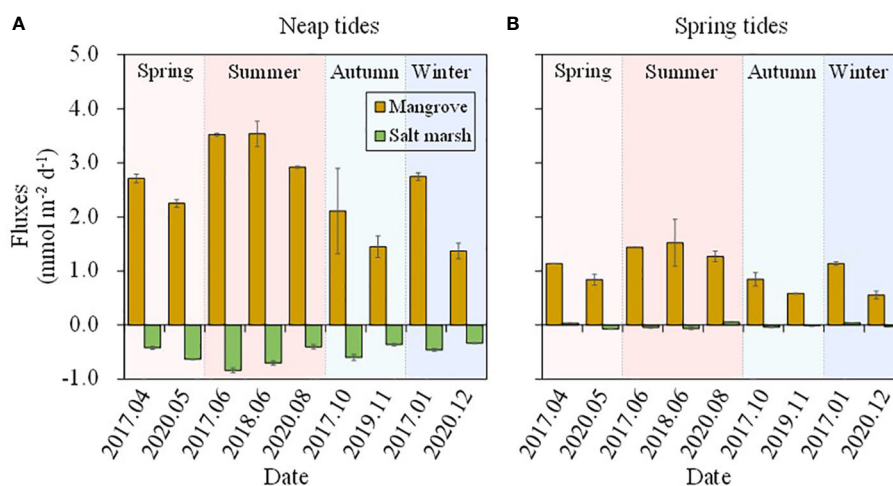

FIGURE 6
Estimated vertical fluxes of DSi during neap tides **(A)** and spring tides **(B)** based on the seasonal observations in mangrove and salt marsh creek during 2017-2020.

TABLE 3 The horizontal, vertical and total fluxes of DSi across the mangroves, salt marshes and tidal creek interface. The positive and negative values indicate the efflux of groundwater and influx of surface water, respectively.

Tidal types	Habitats	Flux types	F (mmol m^{-2} h^{-1})
Neap tides	Mangrove	Horizontal	0.64
		Vertical	2.11
		Total	2.75
	Salt marsh	Horizontal	0.39
		Vertical	-0.38
		Total	0.01
Spring tides	Mangrove	Horizontal	0.83
		Vertical	2.40
		Total	3.23
	Salt marsh	Horizontal	0.11
		Vertical	-0.06
		Total	0.05

4.4 Environmental implications

Not only the nutrient concentration but the nutrient stoichiometry often changes algal cell growth, phytoplankton diversity and abundance, affecting the health of marine ecosystems (Humborg et al., 1997; Garnier et al., 2010; Lin and Lin, 2022). The ratios of DSi : DIN and DSi : DRP observed in this study fell well within the range observed in other estuarine systems (Table 4). However, the observed ratios in the groundwater were larger than in most other studies except for DSi : DIN in Pearl River Estuary, Laizhou Bay and Yeongil Bay. The ratios are much higher than the theoretical Redfield ratio (Si:N:P=16:16:1) (Painter et al., 2017; Wang et al., 2003), suggesting Si is not limiting relative to nitrogen and phosphorus in the study area.

The discharge of aquaculture and domestic wastewater with high nutrients has been a crucial disturbance to the wetland-estuarine system. Excess nitrogen and phosphorus inputs over DSi will decrease the ratios of DSi : DIN and DSi : DRP, leading to a brief frenzy of undesirable algal growth and eutrophication (Billen and Garnier, 1997; Conley, 1999). The groundwater with high DSi concentrations, large DSi : DIN and DSi : DRP ratios was exported from the wetlands to the estuary (Table 2), increasing the contribution to preventing eutrophication in coastal water.

Damming alters the hydrodynamic conditions of the channel, extends the hydraulic retention time, and increases the diatom biomass, thus reducing DSi concentration in downstream (Beusen et al., 2009). The observed results in the Zhangjiang river showed that DSi concentrations in the upper reach of the dam were 9-34% larger than that in the lower reach (Table S2), which suggested the retention of DSi and the decrease in DSi flux from land to ocean. Though nitrogen and phosphorus also can be trapped by dams, the discharge of them caused by the human activities in downstream could compensate for or even exceed the amount of retention (Ittekkot et al., 2000). Nevertheless, there was no compensation to

DSi. As a result, the diatoms are increasingly outcompeted by the harmful algaes that do not require silicon to grow. Large export of DSi from the wetlands has the potential to mitigate the negative effects (e.g. eutrophication) on marine ecosystem health caused by dams. Given the large number of dams in operation (Grill et al., 2015; Mailhot et al., 2018), the assessments of the resulting DSi retention and the role of wetlands in alleviating the retention have a great significance in the management and restoration of wetlands at global scales.

The alterations in vegetation habitats had a significant impact on nutrient cycling and transport across the coastal area to the ocean (Carey and Fulweiler, 2014). Nevertheless, DSi fluxes in the salt marshes were one or two orders of magnitude lower than in the mangroves, indicating the salt marshes played a minor role in regulating DSi exchange between wetlands and coastal water in our study. Additional observations in other regional or global scales are needed to evaluate the effects of salt marsh invasion or mangrove expansion on DSi export from the coastal wetlands, which were scarcely studied.

5 Conclusions

A combination of spatial comparative study, time-series observations, and hydrological identification was used to explore DSi export-import pattern in a mangrove-salt marsh creek-estuary continuum in southeast China. The DSi spatial (mangrove-salt marsh creek-estuary) and temporal (flood-ebb tides) distributions, and the fluxes across the SWI revealed the mangroves had a net DSi export due to large DSi concentrations in groundwater and larger groundwater outflow than surface water inflow. The salt marshes had a net DSi import due to low DSi concentrations in groundwater and low groundwater outflow rates, half that of surface water inflow rates. Lower pH caused by high contents of sulfur and tannin,

TABLE 4 Comparisons of DSi : DIN and DSi : DRP ratios in surface water (SW) and groundwater (GW) with previous estuarine studies.

Study area	Types	DSi : DIN	DSi : DRP	Year	Reference
Pearl River Estuary, China	SW	2.80	115	2006	Tao et al. (2021)
Pearl River Estuary, China	SW	1.21	63	2008	Tao et al. (2021)
Pearl River Estuary, China	SW	1.12	60	2016	Tao et al. (2021)
Changjiang River Estuary, China	SW	0.73	490	2017	Chen et al. (2021)
Jiaozhou Bay, China	SW	0.23-0.45	5-36	2016	Zhang et al. (2020)
Dan'ao River, China	SW	0.15-2.17	11.00	2016	Xiao et al. (2019)
Global scale	SW	1.59	56	–	Cho et al. (2018)
Dan'ao Estuary, China	SW	0.41 ± 0.29	4 ± 3	2015	Li et al. (2018)
Changjiang River Estuary, China	SW	1.17	106	2014	Liang and Xian (2018)
Laizhou Bay, China	SW	3.10	107	2012	Zhang and Gao (2016)
Jiulong Estuary, China	SW	1.07 ± 0.18	135 ± 40	2008-2011	Yan et al. (2012)
Yeongil Bay, Korea	SW	5.52	100	2004	Kim et al. (2008)
Yeoja Bay, Korea	SW	0.37	36.00	2003	Hwang et al. (2005)
Coleroon river estuary, India	GW	0.32	4	2016	Prakash et al. (2021)
Bohai Bay, China	GW	1.19	63	2017	Wang et al. (2020)
Dan'ao River, China	GW	0.38	26	2016	Xiao et al. (2019)
Shengsi Island, East China Sea	GW	0.88	71	2015	Chen et al. (2019)
Global scale	GW	3.19	128	–	Cho et al. (2018)
Daya Bay, China	GW	2.73	154	2013	Wang et al. (2018)
Maowei Sea, China	GW	2.09	177	2016	Chen et al. (2019)
Sanggou Bay, Shandong, China	GW	0.05	15	2012	Wang et al. (2014)
Yeongil Bay, Korea	GW	0.07-0.58	97-633	2004	Kim et al. (2008)
Tampa Bay, USA	GW	0.86-1.15	448	2006	Kroeger et al. (2007)
Yeoja Bay, Korea	GW	0.06-9	38-1122	2003	Hwang et al. (2005)
Zhangjiang Estuary-wetland	SW	1.9 ± 0.2	88 ± 53	2020	This study
Zhangjiang Estuary-wetland	GW	3.0 ± 1.4	1108 ± 758	2020	This study

The concentrations of DIN and DRP is derived from Wang et al. 2022b.

higher temperature caused by shorter inundation time, lower absorption capacity of plants, and larger hydraulic gradient in the mangroves explained larger DSi export than the salt marshes. The DSi export-import pattern suggested the mangroves served as the source of DSi while the salt marshes served as the sink. Two orders of magnitude lower influxes in the salt marshes than the effluxes in the mangroves indicated the salt marsh invasion would not change the source function of the native wetlands. The study provides new insights into the potential ecological implications of the ongoing salt marsh invasion on mangrove DSi outwelling. Future work on other mangrove-salt marsh transition wetlands is suggested to explore the global effects of salt marsh invasions on Si cycles.

The mangrove-salt marsh ecotone had a large DSi : DIN and DSi : DRP ratio up to 3.0 ± 1.4 and 1108 ± 758 in groundwater, respectively. Porewater exchange driving the net export of DSi from

mangroves would modify the nutrient stoichiometry, reduce the eutrophication potential and mitigate the negative effects of reduced river DSi transport caused by damming on the coastal ecosystem.

Data availability statement

The raw data supporting the conclusions of this article will be made available by the authors, without undue reservation.

Author contributions

In this study, FW and NC designed the research and performed data analysis. ZL, YW and RY provided supports for experiments

and data collection. FW, ZL and YW carried out the investigation. The manuscript was prepared and written mainly by FW and NC, with input from all coauthors. All authors contributed to the article and approved the submitted version.

Funding

Acknowledgments

Conflict of interest

The authors declare that the research was conducted in the absence of any commercial or financial relationships that could be construed as a potential conflict of interest.

Publisher's note

Supplementary material

The Supplementary Material for this article can be found online at: https://www.frontiersin.org/articles/10.3389/fmars.2023.1206776/full#supplementary-material

References

Alongi, D. M. (2014). Carbon cycling and storage in mangrove forests. *Ann. Rev. Mar. Sci.* 6, 195–219. doi: 10.1146/annurev-marine-010213-135020

Alongi, D. M. (2020). Carbon balance in salt marsh and mangrove ecosystems: a global synthesis. *J. Mar. Sci. Eng.* 8 (10), 21. doi: 10.3390/jmse8100767

Aoki, Y., Hoshino, M., and Matsubara, T. (2007). Silica and testate amoebae in a soil under pine-oak forest. *Geoderma* 142 (1-2), 29–35. doi: 10.1016/j.geoderma.2007.07.009

Beusen, A. H. W., Bouwman, A. F., Durr, H. H., Dekkers, A. L. M., and Hartmann, J. (2009). Global patterns of dissolved silica export to the coastal zone: results from a spatially explicit global model. *Global Biogeochem. Cycles* 23, 1–13. doi: 10.1029/2008gb003281

Bidle, K. D., and Azam, F. (1999). Accelerated dissolution of diatom silica by marine bacterial assemblages. *Nature* 397 (6719), 508–512. doi: 10.1038/17351

Bidle, K. D., Manganelli, M., and Azam, F. (2002). Regulation of oceanic silicon and carbon preservation by temperature control on bacteria. *Science* 298 (5600), 1980–1984. doi: 10.1126/science.1076076

Billen, G., and Garnier, J. (1997). The phison river plume: coastal eutrophication in response to changes in land use and water management in the watershed. *Aquat. Microbial Ecol.* 13 (1), 3–17. doi: 10.3354/ame013003

Carey, J. C., and Fulweiler, R. W. (2014). Salt marsh tidal exchange increases residence time of silica in estuaries. *Limnol. Oceanog.* 59 (4), 1203–1212. doi: 10.4319/lo.2014.59.4.1203

Chen, X. G., Du, J. Z., Yu, X. Q., and Wang, X. X. (2021). Porewater-derived dissolved inorganic carbon and nutrient fluxes in a saltmarsh of the changjiang river estuary. *Acta Oceanol. Sinica.* 40 (8), 32–43. doi: 10.1007/s13131-021-1797-z

Chen, X. G., Wang, J. L., Cukrov, N., and Du, J. Z. (2019). Porewater-derived nutrient fluxes in a coastal aquifer (Shengsi island, China) and its implication. *Estuar. Coast. Shelf Sci.* 218, 204–211. doi: 10.1016/j.ecss.2018.12.019

Chen, N. W., Wu, Y. Q., Wu, J. Z., Yan, X. L., and Hong, H. S. (2014). Natural and human influences on dissolved silica export from watershed to coast in southeast China. *J. Geophys. Research-Biogeosci.* 119 (1), 95–109. doi: 10.1002/2013jg002429

Cho, H. M., Kim, G., Kwon, E. Y., Moosdorf, N., Garcia-Orellana, J., and Santos, I. R. (2018). Radium tracing nutrient inputs through submarine groundwater discharge in the global ocean. *Sci. Rep.* 8, 1–7. doi: 10.1038/s41598-018-20806-2

Coluccio, K. M., Santos, I. R., Jeffrey, L. C., and Morgan, L. K. (2021). Groundwater discharge rates and uncertainties in a coastal lagoon using a radon mass balance. *J. Hydrol.* 598, 15. doi: 10.1016/j.jhydrol.2021.126436

Conley, D. J. (1999). Biogeochemical nutrient cycles and nutrient management strategies, developments in hydrobiology; man and river systems: the functioning of

river systems at the basin scale. *Develop. Hydrobiol.* pp, 87–96. doi: 10.1023/A:1003784504005

Cornelis, J. T., Delvaux, B., Georg, R. B., Lucas, Y., Ranger, J., and Opfergelt, S. (2011). Tracing the origin of dissolved silicon transferred from various soil-plant systems towards rivers: a review. *Biogeosciences* 8 (1), 89–112. doi: 10.5194/bg-8-89-2011

Cornelis, J. T., Ranger, J., Iserentant, A., and Delvaux, B. (2010). Tree species impact the terrestrial cycle of silicon through various uptakes. *Biogeochemistry* 97 (2-3), 231–245. doi: 10.1007/s10533-009-9369-x

de Bakker, N. V. J., Hemminga, M. A., and Van Soelen, J. (1999). The relationship between silicon availability, and growth and silicon concentration of the salt marsh halophyte spartina anglica. *Plant Soil.* 215 (1), 19–27. doi: 10.1023/a:1004751902074

Delgard, M. L., Deflandre, B., Metzger, E., Nuzzio, D., Capo, S., Mouret, A., et al. (2012). *In situ* study of short-term variations of redox species chemistry in intertidal permeable sediments of the arcachon lagoon. *Hydrobiologia* 699 (1), 69–84. doi: 10.1007/s10750-012-1154-5

Elizondo, E. B., Carey, J. C., Al-Haj, A. N., Lugo, A. E., and Fulweiler, R. W. (2021). High productivity makes mangroves potentially important players in the tropical silicon cycle. *Front. Mar. Sci.* 8. doi: 10.3389/fmars.2021.652615

Epstein, E. (1994). The anomaly of silicon in plant biology. *Proc. Natl. Acad. Of Sci. Of United States Of America* 91 (1), 11–17. doi: 10.1073/pnas.91.1.11

Epstein, E. (2001). "Silicon in plants: facts vs. concepts," *In Studies in plant science*. Elsevier 8, 1–15. doi: 10.1016/S0928-3420(01)80005-7

Ferreira, T. O., Otero, X. L., Vidal-Torrado, P., and Macias, F. (2007). Effects of bioturbation by root and crab activity on iron and sulfur biogeochemistry in mangrove substrate. *Geoderma* 142, 36–46. doi: 10.1016/j.geoderma.2007.07.010

Gao, G. F., Li, P. F., Shen, Z. J., Qin, Y. Y., Zhang, X. M., Ghoto, K., et al. (2018). Exotic spartina alterniflora invasion increases CH_4 while reduces CO_2 emissions from mangrove wetland soils in southeastern China. *Sci. Rep.* 8 (1), 9243. doi: 10.1038/s41598-018-27625-5

Garnier, J. A., Mounier, E. M., Laverman, A. M., and Billen, G. F. (2010). Potential denitrification and nitrous oxide production in the sediments of the Seine River drainage network (France). *J Environ Qual.* 39 (2), 449–459. doi: 10.2134/jeq2009.0299

Gong, Z. T., and Zhang, X. P. (1994). Mangrove and acid sulphate soils in China (in Chinese). *Acta Pedol Sin.* 1), 86–94. doi: CNKI:SUN:TRXB.0.1994-01-010

Grill, G., Lehner, B., Lumsdon, A. E,p MacDonald, G. K., Zarfl, C., and Liermann, C. R. (2015). An index-based framework for assessing patterns and trends in river fragmentation and flow regulation by global dams at multiple scales. *Environ. Res. Lett.* 10 (1), 15001. doi: 10.1088/1748-9326/10/1/015001

Harrison, J. A., Frings, P. J., Beusen, A. H. W., Conley, D. J., and McCrackin, M. L. (2012). Global importance, patterns, and controls of dissolved silica retention in lakes and reservoirs. *Global Biogeochem. Cycles.* 26 (2), 1–12. doi: 10.1029/2011GB004228

Hodson, M. J., White, P. J., Mead, A., and Broadley, M. R. (2005). Phylogenetic variation in the silicon composition of plants. *Ann. Bot-london.* 96 (6), 1027–1046. doi: 10.1093/aob/mci255

Hou, L. J., Liu, M., Yang, Y., Ou, D. N., Lin, X., and Chen, H. (2010). Biogenic silica in intertidal marsh plants and associated sediments of the Yangtze estuary. *J. Environ. Sci.* 22 (3), 374–380. doi: 10.1016/s1001-0742(09)60118-2

Hu, M. J., Sardans, J., Le, Y. X., Yan, R. B., Zhong, Y., Huang, J. F., et al. (2022). Biogeochemical behavior of p in the soil and porewater of a low-salinity estuarine wetland: availability, diffusion kinetics, and mobilization mechanism. *Water Res.* 219, 118617. doi: 10.1016/j.watres.2022.118617

Hughes, C. E., Binning, P., and Willgoose, G. R. (1998). Characterisation of the hydrology of an estuarine wetland. *J. Hydrol.* 211 (1-4), 34–49. doi: 10.1016/s0022-1694(98)00194-2

Humborg, C., Ittekkot, V., Cociasu, A., and Bodungen, B.v. (1997). Effect of danube river dam on black sea biogeochemistry and ecosystem structure. *Nature* 386 (6623), 385–388. doi: 10.1038/386385a0

Hwang, D. W., Kim, G. B., Lee, Y. W., and Yang, H. S. (2005). Estimating submarine inputs of groundwater and nutrients to a coastal bay using radium isotopes. *Mar. Chem.* 96 (1-2), 61–71. doi: 10.1016/j.marchem.2004.11.002

Ittekkot, V., Humborg, C., and Schafer, P. (2000). Hydrological alterations and marine biogeochemistry: a silicate issue? *Bioscience* 50 (9), 776–782. doi: 10.1641/0006-3568(2000)050[0776:Haamba]2.0.Co;2

Jin, L., Lu, C. Y., Ye, Y., and Ye, G. F. (2013). Soil respiration in a subtropical mangrove wetland in the jiulong river estuary, China. *Pedosphere* 23 (5), 678–685. doi: 10.1016/S1002-0160(13)60060-0

Kellermeier, M., Gebauer, D., Melero-Garcia, E., Drechsler, M., Talmon, Y., Kienle, L., et al. (2012). Colloidal stabilization of calcium carbonate prenucleation clusters with silica. *Advanced Funct. Materials.* 22 (20), 4301–4311. doi: 10.1002/adfm.201200953

Kim, G., Ryu, J. W., and Hwang, D. W. (2008). Radium tracing of submarine groundwater discharge (SGD) and associated nutrient fluxes in a highly-permeable bed coastal zone, Korea. *Mar. Chem.* 109 (3-4), 307–317. doi: 10.1016/j.marchem.2007.07.002

Kroeger, K. D., Swarzenski, P. W., Greenwood, W. J., and Reich, C. (2007). Submarine groundwater discharge to Tampa bay: nutrient fluxes and biogeochemistry of the coastal aquifer. *Mar. Chem.* 104 (1), 85–97. doi: 10.1016/j.marchem.2006.10.012

Lara, M., Peralta, G., Alonso, J. J., Morris, E. P., Gonzalez-Ortiz, V., Rueda-Marquez, J. J., et al. (2012). Effects of intertidal seagrass habitat fragmentation on turbulent diffusion and retention time of solutes. *Mar. pollut. Bulletin.* 64 (11), 2471–2479. doi: 10.1016/j.marpolbul.2012.07.044

Laruelle, G. G., Roubeix, V., Sferratore, A., Brodherr, B., Ciuffa, D., Conley, D. J., et al. (2009). Anthropogenic perturbations of the silicon cycle at the global scale: key role of the land-ocean transition. *Global Biogeochem. Cycles.* 23, 1–17. doi: 10.1029/2008gb003267

Li, D. D., Dong, M. F., Liu, S. M., Chen, H. T., and Yao, Q. Z. (2019). Distribution and budget of biogenic silica in the Yangtze estuary and its adjacent sea. *Sci. Total Environment.* 669, 590–599. doi: 10.1016/j.scitotenv.2019.03.144

Li, G., Li, H. L., Wang, X. J., Qu, W. J., Zhang, Y., Xiao, K., et al. (2018). Groundwater-surface water exchanges and associated nutrient fluxes in dan'ao estuary, daya bay, China. *Continental Shelf Res.* 166, 83–91. doi: 10.1016/j.csr.2018.06.014

Li, B., Liao, C. H., Zhang, X. D., Chen, H. L., Wang, Q., Chen, Z. Y., et al. (2009). Spartina alterniflora invasions in the Yangtze river estuary, China: an overview of current status and ecosystem effects. *Ecol. Engineer.* 35 (4), 511–520. doi: 10.1016/j.ecoleng.2008.05.013

Liang, Y., Nikolic, M., Bélanger, R., Gong, H., and Song, A. (2015). Silicon biogeochemistry and bioavailability in soil, silicon in agriculture: from theory to practice. *Springer Netherlands Dordrecht* pp, 45–68. doi: 10.1007/978-94-017-9978-2_3

Liang, C., and Xian, W. W. (2018). Changjiang nutrient distribution and transportation and their impacts on the estuary. *Continental Shelf Res.* 165, 137–145. doi: 10.1016/j.csr.2018.05.001

Lin, G. M., and Lin, X. B. (2022). Bait input altered microbial community structure and increased greenhouse gases production in coastal wetland sediment. *Water Res.* 218 (3), 118520. doi: 10.1016/j.watres.2022.118520

Liu, J. A., Hrustic, E., Du, J. Z., Gasparovic, B., Cankovic, M., Cukrov, N., et al. (2019). Net submarine groundwater-derived dissolved inorganic nutrients and carbon input to the oligotrophic stratified karstic estuary of the krka river (Adriatic Sea, Croatia). *J. Geophys. Research-Oceans.* 124 (6), 4334–4349. doi: 10.1029/2018jc014814

Liu, Y., Jiao, J. J., and Liang, W. Z. (2018). Tidal fluctuation influenced physicochemical parameter dynamics in coastal groundwater mixing zone. *Estuar. coasts.* 41 (4), 988–1001. doi: 10.1007/s12237-017-0335-x

Liu, Y., Jiao, J. J., Liang, W., and Luo, X. (2017). Tidal pumping-induced nutrients dynamics and biogeochemical implications in an intertidal aquifer. *J. Geophys. Res.: Biogeosci.* 122 (12), 3322–3342. doi: 10.1002/2017JG004017

Ma, J. F., and Takahashi, E. (2002). *Soil, fertilizer, and plant silicon research in Japan* (Amsterdam: Elsevier).

Ma, J. F., and Takahashi, E. (2004). Effect of silicon on the growth and phosphorus uptake of rice. *Plant Soil.* 126, 115–119. doi: 10.1007/BF00041376

Maavara, T., Akbarzadeh, Z., and Van Cappellen, P. (2020a). Global dam-driven changes to riverine n:P:Si ratios delivered to the coastal ocean. *Geophys. Res. Lett.* 47 (15), e2020GL088288. doi: 10.1029/2020GL088288

Maavara, T., Chen, Q. W., Van Meter, K., Brown, L. E., Zhang, J. Y., Ni, J. R., et al. (2020b). River dam impacts on biogeochemical cycling. *Nat. Rev. Earth Environment.* 1 (2), 103–116. doi: 10.1038/s43017-019-0019-0

Maavara, T., Durr, H. H., and Van Cappellen, P. (2014). Worldwide retention of nutrient silicon by river damming: from sparse data set to global estimate. *Global Biogeochem. Cycles.* 28 (8), 842–855. doi: 10.1002/2014gb004875

Mailhot, A., Talbot, G., Ricard, S., Turcotte, R., and Guinard, K. (2018). Assessing the potential impacts of dam operation on daily flow at ungauged river reaches. *J. Hydrology-Regional Stud.* 18, 156–167. doi: 10.1016/j.ejrh.2018.06.006

Millar, D. J., Cooper, D. J., and Ronayne, M. J. (2018). Groundwater dynamics in mountain peatlands with contrasting climate, vegetation, and hydrogeological setting. *J. Hydrol.* 561, 908–917. doi: 10.1016/j.jhydrol.2018.04.050

Moore, W. S. (1996). Large Groundwater inputs to coastal waters revealed by 226Ra enrichments. *Nature* 380 (6575), 612–614. doi: 10.1038/380612a0

Mwashote, B. M., and Jumba, I. O. (2002). Quantitative aspects of inorganic nutrient fluxes in the gazi bay (Kenya): implications for coastal ecosystems. *Mar. pollut. Bulletin.* 44 (11), 1194–1205. doi: 10.1016/s0025-326x(02)00176-5

Oh, Y. H., Kim, D. H., Hwane, S., Lee, H., Moon, S. H., Cho, S. Y., et al. (2020). Determining groundwater inflow and Si behavior in a wetland using Rn-222 mass balance and multidisciplinary approach. *J. Hydrol.* 591, 13. doi: 10.1016/j.jhydrol.2020.125575

Painter, S. C., Hartman, S. E., Kivimae, C., Salt, L. A., Clargo, N. M., Daniels, C. J., et al. (2017). The elemental stoichiometry (C, Si, N, P) of the Hebrides shelf and its role in carbon export. *Prog. Oceanog.* 159, 154–177. doi: 10.1016/j.pocean.2017.10.001

Prakash, R., Srinivasamoorthy, K., Gopinath, S., Saravanan, K., and Vinnarasi, F. (2021). Approximation of submarine groundwater discharge and allied nutrient fluxes to the bay of Bengal, India using nutrient mass balance. *Environ. Earth Sci.* 80 (9), 1–22. doi: 10.1007/s12665-021-09669-5

Qin, Y. C., and Weng, H. X. (2006). Silicon release and its speciation distribution in the surficial sediments of the pearl river estuary, China. *Estuar. Coast. Shelf Sci.* 67 (3), 433–440. doi: 10.1016/j.ecss.2005.11.015

Raven, J. A. (2003). Cycling silicon – the role of accumulation in plants. *New Phytologist.* 158 (3), 419–421. doi: 10.1046/j.1469-8137.2003.00778.x

Rickert, D., Schluter, M., and Wallmann, K. (2002). Dissolution kinetics of biogenic silica from the water column to the sediments. *Geochim Cosmochim Acta* 66 (3), 439–455. doi: 10.1016/s0016-7037(01)00757-8

Sadat-Noori, M., and Glamore, W. (2019). Porewater exchange drives trace metal, dissolved organic carbon and total dissolved nitrogen export from a temperate mangrove wetland. *J. Environ. Manag.* 248, 1–11. doi: 10.1016/j.jenvman.2019.109264

Santos, I. R., Bryan, K. R., Pilditch, C. A., and Tait, D. R. (2014). Influence of porewater exchange on nutrient dynamics in two new Zealand estuarine intertidal flats. *Mar. Chem.* 167, 57–70. doi: 10.1016/j.marchem.2014.04.006

Santos, I. R., Chen, X. G., Lecher, A. L., Sawyer, A. H., Moosdorf, N., Rodellas, V., et al. (2021). Submarine groundwater discharge impacts on coastal nutrient biogeochemistry. *Nat. Rev. Earth Environment.* 2 (5), 307–323. doi: 10.1038/s43017-021-00152-0

Saintilan, N., Wilson, N. C., Rogers, K., Rajkaran, A., and Krauss, K. W. (2014). Mangrove expansion and salt marsh decline at mangrove poleward limits. *Global Change Biol.* 20 (1), 147–157. doi: 0.1111/gcb.12341

Santos, I. R., Maher, D. T., Larkin, R., Webb, J. R., and Sanders, C. J. (2019). Carbon outwelling and outgassing vs. burial in an estuarine tidal creek surrounded by mangrove and saltmarsh wetlands. *Limnol. Oceanog.* 64 (3), 996–1013. doi: 10.1002/lno.11090

Sartor, L. R., Graham, R. C., Ying, S. C., Andrade, G. R. P., Montes, C. R., and Ferreira, T. O. (2019). Are hypersaline tidal flat soils potential silicon sinks in coastal wetlands? *Geoderma* 337, 215–224. doi: 10.1016/j.geoderma.2018.08.028

Sauer, D., Saccone, L., Conley, D. J., Herrmann, L., and Sommer, M. (2006). Review of methodologies for extracting plant-available and amorphous Si from soils and aquatic sediments. *Biogeochemistry* 80 (1), 89–108. doi: 10.1007/s10533-005-5879-3

Street-Perrott, F. A., and Barker, P. A. (2008). Biogenic silica: a neglected component of the coupled global continental biogeochemical cycles of carbon and silicon. *Earth Surface Processes Landforms.* 33 (9), 1436–1457. doi: 10.1002/esp.1712

Struyf, E., and Conley, D. J. (2009). Silica: an essential nutrient in wetland biogeochemistry. *Front. Ecol. Environment.* 7 (2), 88–94. doi: 10.1890/070126

Taniguchi, M. (2002). Tidal effects on submarine groundwater discharge into the ocean. *Geophys. Res. Lett.* 29 (12), 3. doi: 10.1029/2002gl014987

Tao, W., Niu, L. X., Dong, Y. H., Fu, T., and Lou, Q. S. (2021). Nutrient pollution and its dynamic source-sink pattern in the pearl river estuary (south china). *Front. Mar. Sci.* 8. doi: 10.3389/fmars.2021.713907

Wang, X. L., Baskaran, M., Su, K. J., and Du, J. Z. (2018). The important role of submarine groundwater discharge (SGD) to derive nutrient fluxes into river dominated ocean margins-the East China Sea. *Mar. Chem.* 204, 121–132. doi: 10.1016/j.marchem.2018.05.010

Wang, F. F., Chen, N. W., Yan, J., Lin, J. J., Guo, W. D., Cheng, P., et al. (2019). Major processes shaping mangroves as inorganic nitrogen sources or sinks: insights from a multidisciplinary study. *J. Geophys. Research-Biogeosci.* 124 (5), 1194–1208. doi: 10.1029/2018jg004875

Wang, F. F., Cheng, P., Chen, N. W., and Kuo, Y. M. (2021). Tidal driven nutrient exchange between mangroves and estuary reveals a dynamic source-sink pattern. *Chemosphere* 270, 10. doi: 10.1016/j.chemosphere.2020.128665

Wang, X. L., Du, J. Z., Ji, T., Wen, T. Y., Liu, S. M., and Zhang, J. (2014). An estimation of nutrient fluxes *via* submarine groundwater discharge into the sanggou bay-a typical multi-species culture ecosystem in China. *Mar. Chem.* 167, 113–122. doi: 10.1016/j.marchem.2014.07.002

Wang, Q., Li, H., Zhang, Y., Wang, X., Xiao, K., Zhang, X., et al. (2020). Submarine groundwater discharge and its implication for nutrient budgets in the western bohai bay, China. *J. Environ. Radioactivity.* 212, 106132. doi: 10.1016/j.jenvrad.2019.106132

Wang, B., and Lin, X. B. (2023). Exotic spartina alterniflora invasion enhances sediment n-loss while reducing n retention in mangrove wetland. *Geoderma* 431 (7), 116362. doi: 10.1016/j.geoderma.2023.116362

Wang, F. F., Song, A., Zhang, Y., Lin, X. B., Yan, R. F., Wang, Y., et al. (2022a). Saltmarsh sediments with wastewater input emit more carbon greenhouse gases but less N_2O than mangrove sediments. *CATENA* 213, 106205. doi: 10.1016/j.catena.2022.106205

Wang, G. Z., Wang, Z. Y., Zhai, W. D., Moore, W. S., Li, Q., Yan, X. L., et al. (2015). Net subterranean estuarine export fluxes of dissolved inorganic C, N, P, Si, and total alkalinity into the jiulong river estuary, China. *Geochim. Et Cosmochim. Acta* 149, 103–114. doi: 10.1016/j.gca.2014.11.001

Wang, B. D., Wang, X. L., and Zhan, R. (2003). Nutrient conditions in the yellow Sea and the East China Sea. *Estuar. Coast. Shelf Sci.* 58 (1), 127–136. doi: 10.1016/s0272-7714(03)00067-2

Wang, F. F., Xiao, K., Santos, I. R., Lu, Z. Y., Tamborski, J., Wang, Y., et al. (2022b). Porewater exchange drives nutrient cycling and export in a mangrove-salt marsh ecotone. *J. Hydrol.* 606, 11. doi: 10.1016/j.jhydrol.2021.127401

Xia, S. P., Song, Z. L., Van Zwieten, L., Guo, L. D., Yu, C. X., Hartley, I. P., et al. (2020). Silicon accumulation controls carbon cycle in wetlands through modifying nutrients stoichiometry and lignin synthesis of phragmites australis. *Environ. Exp. Botany.* 175, 11. doi: 10.1016/j.envexpbot.2020.104058

Xiao, K., Li, G., Li, H. L., Zhang, Y., Wang, X. J., Hu, W. L., et al. (2019). Combining hydrological investigations and radium isotopes to understand the environmental effect of groundwater discharge to a typical urbanized estuary in China. *Sci. Total Environment.* 695, 1–15. doi: 10.1016/j.scitotenv.2019.133872

Xiao, K., Li, H. L., Wilson, A. M., Xia, Y. Q., Wan, L., Zheng, C. M., et al. (2017). Tidal groundwater flow and its ecological effects in a brackish marsh at the mouth of a large sub-tropical river. *J. Hydrol.* 555, 198–212. doi: 10.1016/j.jhydrol.2017.10.025

Yan, X. L., Zhai, W. D., Hong, H. S., Li, Y., Guo, W. D., and Huang, X. (2012). Distribution, fluxes and decadal changes of nutrients in the jiulong river estuary, southwest Taiwan strait. *Chin. Sci. Bulletin.* 7 (18), 2307–2318. doi: 10.1007/s11434-012-5084-4

Yang, J. L., and Zhang, G. L. (2018). Silicon cycling by plant and its effects on soil Si translocation in a typical subtropical area. *Geoderma* 310, 89–98. doi: 10.1016/j.geoderma.2017.08.014

Zhang, J. F., and Gao, X. L. (2016). Nutrient distribution and structure affect the acidification of eutrophic ocean margins: a case study in southwestern coast of the laizhou bay, China. *Mar. pollut. Bulletin.* 111 (1-2), 295–304. doi: 10.1016/j.marpolbul.2016.06.095

Zhang, Y. H., Huang, G. M., Wang, W. Q., Chen, L. Z., and Lin, G. H. (2012). Interactions between mangroves and exotic spartina in an anthropogenically disturbed estuary in southern China. *Ecology* 93 (3), 588–597. doi: 10.1890/11-1302.1

Zhang, Q. F., and Laanbroek, H. J. (2020). Tannins from senescent rhizophora mangle mangrove leaves have a distinctive effect on prokaryotic and eukaryotic communities in a distichlis spicata salt marsh soil. *FEMS Microbiol. Ecol.* 96 (9). doi: 10.1093/femsec/fiaa148

Zhang, Y., Santos, I. R., Li, H. L., Wang, Q. Q., Xiao, K., Guo, H. M., et al. (2020). Submarine groundwater discharge drives coastal water quality and nutrient budgets at small and large scales. *Geochim Cosmochim Acta* 290, 201–215. doi: 10.1016/j.gca.2020.08.026

Zhou, H. C., Wei, S. D., Zeng, Q., Zhang, L. H., Tam, N. F. Y., Lin, Y. M., et al. (2010). Nutrient and caloric dynamics in Avicennia marina leaves at different developmental and decay stages in Zhangjiang River Estuary, China. *Estuar. Coast. Shelf Sci.* 87 (1), 21–26. doi: 10.1016/j.ecss.2009.12.005